Responses of groundwater vulnerability to artificial recharge under extreme weather conditions in Shijiazhuang City, China

Xiaosi Su, Wei Xu and Shanghai Du

ABSTRACT

Artificial recharge is becoming one of the most important ways to deal with water shortage and induced environmental geological problems, but it also brings potential groundwater contaminant risks, especially under extreme weather conditions. A classic method, DRASTIC, and groundwater flow simulation model have been used to analyze the response of groundwater vulnerability to artificial recharge under extreme weather conditions. The results show that a simultaneously abundant year and scarce year of the local area and the Han River Basin are 7.46 and 6.60%, respectively. The quantities of artificial recharge water would be 8.72×10^4 m^3/a and 4.64×10^4 m^3/a, respectively. Five scenarios with extreme weather conditions were discussed. The groundwater vulnerability would not change a great deal without extreme conditions under artificial recharge. Under extreme abundant conditions, the induced groundwater level lowering would making the depth of groundwater level increase, and the vulnerability would be lower. Under extreme abundant conditions, the decreased depth of groundwater level and increased net recharge made the vulnerability increase obviously, and the low vulnerability area was converted into the moderate and high vulnerability areas. More attention should be paid to the quality of recharged water and monitoring schemes should be carried out around the infiltration field.

Key words | artificial recharge, DRASTIC, extreme weather conditions, groundwater reservoir, groundwater vulnerability, Hutuo River

Xiaosi Su
Wei Xu
Shanghai Du (corresponding author)
Key Laboratory of Groundwater Resources and Environment,
Ministry of Education,
Jilin University; Institute of Water Resources and Environment,
Jilin University,
2519-Jiefang Road,
Changchun, 130026,
China
E-mail: *yoko_sh@yeah.net*

INTRODUCTION

Artificial recharge is becoming one of the most important ways to deal with the problems of groundwater level depression, seawater intrusion, and land subsidence (Bouwer 2002; Dong *et al.* 2013; Du *et al.* 2013). Although artificial recharge could solve environmental geological issues, the variations of groundwater flow condition change the groundwater defense capacity of pollution significantly. Research into groundwater vulnerability responses to different artificial recharge plans would be very useful for making decisions about groundwater artificial recharge plans and groundwater resources management (Robins 1998; Sundaram *et al.* 2008; Iqbal *et al.* 2012).

Groundwater vulnerability refers to the sensitivity of groundwater systems to pollution, which means the possibilities and trends of groundwater under the joint actions of inherent properties and environmental factors (Iqbal *et al.* 2012). Because of its clear evaluation purpose, simple usage and easily obtained data, the DRASTIC method has become the most popular method for groundwater vulnerability evaluation, especially after the joint usage of GIS (Geographic Information System) technology (Baalousha 2006; Bai *et al.* 2012; Iqbal *et al.* 2012). According to the literature search results, many improved methods used in the study of different groundwater vulnerability analyses have been proposed based on different purposes and study

doi: 10.2166/aqua.2013.132

areas (Barbash & Resek 1996; Worrall & Kolpin 2004). The consistency of groundwater contamination status with groundwater vulnerability results has been discussed recently (Ramos *et al.* 2012), and the sensitivity analysis of groundwater vulnerability with single factors has also been reported (Huan *et al.* 2012), but there is little literature discussing the impacts of human activities on groundwater vulnerability. For example, agricultural irrigation with groundwater would enhance the thickness of the vadose zone, and the infiltration of irrigation could enhance the quantity of net recharge, which could impact groundwater vulnerability according to the evaluation method. The research into groundwater vulnerability responses to human activities is the study of groundwater vulnerability variations under the condition of multi-factor simultaneous changes (Saidi *et al.* 2011; Aschonitis *et al.* 2012; Chen *et al.* 2013; Zhai *et al.* 2013).

Groundwater reservoir (GR) is a popular water resources management method in China, and refers to water conservation in available porous media under artificial control for water storage and exploitation (Li 2007; Du *et al.* 2013). The Hutuo Groundwater Reservoir (HGR) located at Shijiazhuang City, China, and the transferred water from the Han River (HR) and local surplus water from the upstream reservoir in the flood season are the main water sources for the HGR, with the water able to be recharged through an abandoned river bed. The recharged water would change the local groundwater level and net recharge of the infiltration field, and the groundwater vulnerability could be changed a great deal correspondingly. Additionally, the local surplus water from the upstream surface water reservoir and the transferred water from HR are controlled by local weather conditions and that of HR, respectively. The occurrence of extreme weather conditions and their encounters between the local area and HR could produce a big change in the quantities for recharge; the groundwater vulnerability could be changed by the extreme weather conditions. In this study, the classic DRASTIC evaluation method and groundwater flow simulation based on the GMS model have been jointly used, and the responses of groundwater vulnerability to extreme weather conditions are discussed.

STUDY AREA

Shijiazhuang is the capital of Hebei Province, China (Figure 1), and is located on the alluvial fan of the Hutuo River. The local reservoir, the Huangbizhuang Reservoir, is located at the outlet of the HR rising in the Taihang Mountain, and is the most important hydraulic project in Shijiazhuang. The bed of the HR below the reservoir is dry all year, except during the flood season when it receives surplus water from the local reservoir. The main components of the water transfer network in the area are the Shijin, Yuanquan, Dongming, Ximing and main channels of South-to-North Transfer Water Project. The main channel of the South-to-North Transfer Water Project was constructed with the aim of resolving water shortage problems in Beijing and the surrounding area. This channel is 1,273 km long. According to the South-to-North Transfer Water Project plan, $130 \times 10^8\ m^3$ of surface water could be transferred from the Yangtze River to Beijing and other cities, including Shijiazhuang.

There are two layers in the quaternary aquifer. The upper layer is Holocene-upper and middle Pleistocene phreatic aquifer, which is the dominant aquifer used to supplement the water supply of Shijiazhuang. The lower layer is lower Pleistocene confined aquifer, and is separated from the upper layer by a section of continuous clay. The local hydrology, geology and hydrogeological conditions are discussed in detail in Du *et al.* (2013). An *in situ* infiltration test was done to calculate the infiltration rate, discussed in detail in Su *et al.* (2013), and these results show the following.

(1) There would be $4.64–8.72 \times 10^8\ m^3/a$ of water that could be used as water source for artificial recharge under different abundance and scarce encountering (Du *et al.* 2013).
(2) The total storage capacity of the HGR was calculated at $106.30 \times 10^8\ m^3$, and the dewatering capacity was calculated as $33.51 \times 10^8\ m^3$, and this demonstrates that the cone of depression has a large water storage space to accommodate artificial recharge (Du *et al.* 2013).
(3) A field-scale infiltration test was carried out to solve the problem of infiltration rate at the infiltration site over 10 days. The total amount of recharge water over this

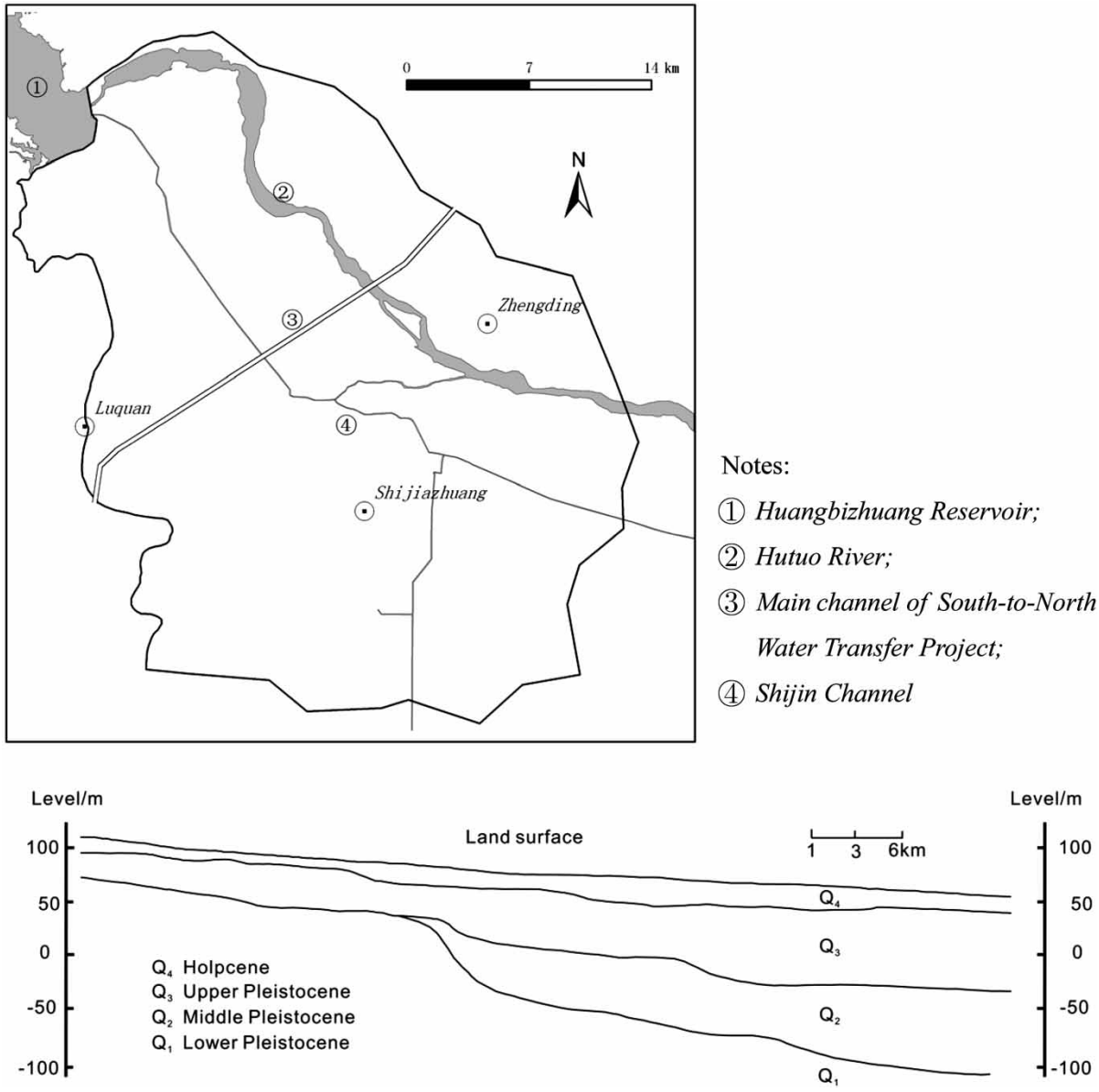

Figure 1 | Location of Shijiazhuang City and the main water bodies and pathways.

period was 1.15×10^7 m^3, the seepage area was about 0.6 km^2, and the steady infiltration rate was about 1.4 m/d (Su *et al.* 2013). Using the infiltration rate of 1.4 m/d, and enlarging the infiltration area to 3 km^2 by digging the central area of the riverbed, we can calculate that about 10–15 $\times 10^8$ m^3 of surface water could be recharged into the HGR. The infiltration capacity of the river bed would be a vital factor impacting the net recharge around the infiltration field and change the groundwater vulnerability around the infiltration field.

(4) The study results of the field-scale infiltration test and the groundwater level prediction based on the simulation models show that the groundwater level would be rapidly and significantly enhanced (Du *et al.* 2013; Su *et al.* 2013), which means that the groundwater vulnerability would be changed due to artificial recharge.

METHODOLOGY AND MATERIALS

A classic method named DRASTIC (Aller *et al.* 1987) has been used to evaluate the groundwater vulnerability, with seven factors used during the evaluation: D – depth to groundwater table, R – recharge, A – aquifer media, S – soil media, T – topography, I – impact of the vadose zone, and C – hydraulic conductivity. The DRASTIC Index (DI) can be calculated based on the equation:

$$DI = D_r D_w + R_r R_w + A_r A_w + S_r S_w + T_r T_w + I_r I_w + C_r C_w$$

where, D_r, R_r, A_r, S_r, T_r, I_r and C_r refer to ratings of the depth to water table, aquifer recharge, aquifer media, soil media, topography, vadose zone, hydraulic conductivity, respectively; D_w, R_w, A_w, S_w, T_w, I_w and C_w refer to weights assigned to the depth to groundwater table, aquifer recharge, aquifer media, soil media, topography, vadose zone, and hydraulic conductivity, respectively. The ratings used in the DRASTIC method are shown in Table 1, and the weights in Table 2.

Depth to the groundwater table (D)

D is thickness of the unsaturated zone. An increase of D affects the residence time of organic pollution and increases the chance of oxidation of organic pollutants; it reduces groundwater organic pollution risks by sorption, biodegradation, dispersion, and volatilization during the migration process. The distribution of the depth to groundwater table depends on the groundwater level and surface elevations. In this study, several scenarios which affect the groundwater level were considered and the distributions of the depth to groundwater table in different scenarios are discussed in the sections below.

Net recharge (R)

R is the quantity of water per unit area that can be infiltrated into an aquifer from the surface. The infiltrated water can transport organic pollutants into the aquifer and form planar pollution associated with migration along with organic pollutants. Increasing R may introduce more organic pollutants into the aquifer, but a relatively large R could dilute these pollutants. The distribution of R depends on regional precipitation, evaporation and land use conditions. Different precipitation frequencies were considered with different scenarios and the distribution of R is discussed in the sections below.

Aquifer material (A)

Aquifer controls the lateral migration path of organic pollutants, and increasing aquifer media particle sizes with greater porosity may enhance dilution capacity. According to the hydrogeological conditions, the distribution of A is shown in Figure 2.

Soil media (S)

Soil media represent a significant factor for influencing groundwater pollution potential. The make-up of soil media on groundwater vulnerability directly impact the amount of recharge and the ability of contaminants to infiltrate the vadose zone. Soil permeability and contaminant migration are directly linked to soil type, shrink and swell potential, and grain size of the soil. According to the test results, the distribution of organic matter in soil is shown in Figure 3.

Topography (T)

T has a direct impact on regional precipitation distribution and the relationship between runoff and infiltration. An increase of T may enhance the infiltration rate of water along with organic pollutants. According to the topography, the distribution of T is shown in Figure 4.

Impact of the vadose zone (I)

Impact of the vadose zone refers to the unsaturated zone that modulates vertical migration of pollutants. The vertical permeability coefficient K can be used in the assessment of groundwater organic pollution. An increase of K may reduce the residence time of pollutants in the unsaturated zone and enhance the concentration of organic pollutants in groundwater. According to geologic conditions in the HGR, the distribution map of impact of the vadose zone is shown in Figure 5.

Table 1 | Ranges and ratings for DRASTIC factors (Aller *et al*. 1987)

D(m)		R (mm)		A		S		T(%)		I		C(m/d)	
Range	**Rating**	**Range**	**Rating**	**Range**	**Rating**	**Range**	**Rating**	**Range**	**Rating**	**Range**	**Rating**	**Range**	**Rating**
> 30.5	1	0–50.8	1	Massive shale	1–3	Thin or absent	10	0–2	10	Silt/Clay	1–2	0.04–4.1	1
26.7–30.5	2	50.8–101.6	3	Metamorphic/ Igneous	2–5	Gravel	10	2–6	9	Shale	2–5	4.1–12.2	2
22.9–26.7	3	101.6–177.8	6	Weathered; Metamorphic/ Igneous	3–5	Sand	9	6–12	5	Limestone	2–7	12.2–28.5	4
15.2–22.9	4	177.8–254	8	Thin bedded sandstone, limestone, shale	5–9	Shrinking/ Aggregated clay	7	12–18	3	Sandstone	4–8	28.5–40.7	6
12.1–15.2	5	> 254	9	Massive sandstone	4–9	Sandy loam	6	> 18	1	Bedded limestone, sandstone, shale sand and gravel with significant silt and clay	4–8	40.7–81.5	8
9.1–12.1	6			Massive limestone	4–9	Loam	5			Silt and clay	4–8	> 81.5	10
6.8–9.1	7			Sand and gravel	4–9	Silty loam	4			Metamorphic/ Igneous	2–8		
4.6–6.8	8			Basalt	2–10	Clay loam	3						
1.5–4.6	9			Karst limestone	9–10	No-shrinking/No-aggregated clay	1						
≤ 1.5	10												

Table 2 | Factor weights used in DRASTIC model (Aller *et al*. 1987)

Factors	D	R	A	S	T	I	C
Weights	5	4	3	2	1	5	3

Hydraulic conductivity (C)

C represents the hydraulic transmission capacity of aquifer media, and controls the migration rate of groundwater and organic pollutants (Qian *et al*. 2009). According to the hydrogeological test results, the distribution of C is shown in Figure 6.

RESULTS AND DISCUSSION

Water sources under extreme weather conditions

In this paper, the annual precipitation from 1956 to 1998 was used to analyze the possibilities of encountering different combinations of abundant or scarce precipitation in the two regions. Nine combinations of either abundant or scarce precipitation in the local area and the transfer water area are shown in Table 3. From the table it can be seen that the simultaneously abundant year of local area and Han River Basin is 7.46% of the years, and 6.60% of the years with a simultaneously scarce year. Both of the

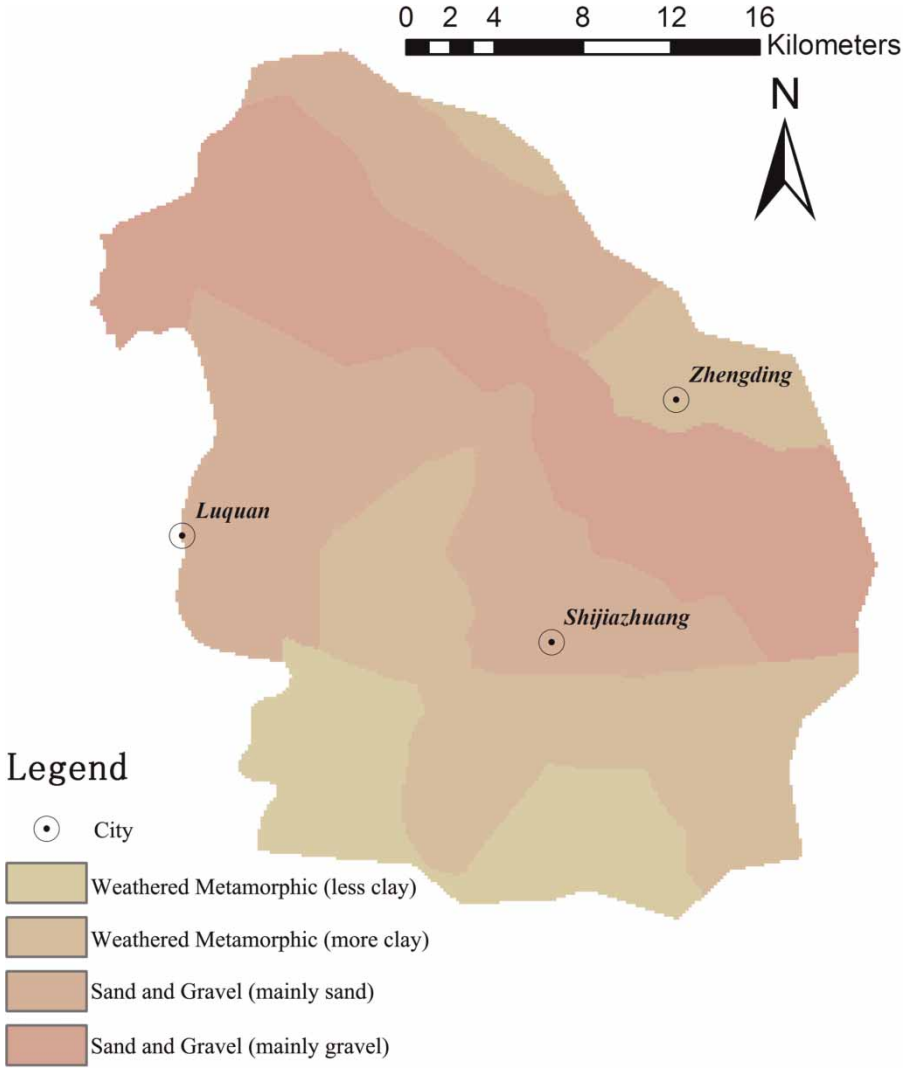

Figure 2 | Aquifer material (A) distribution map.

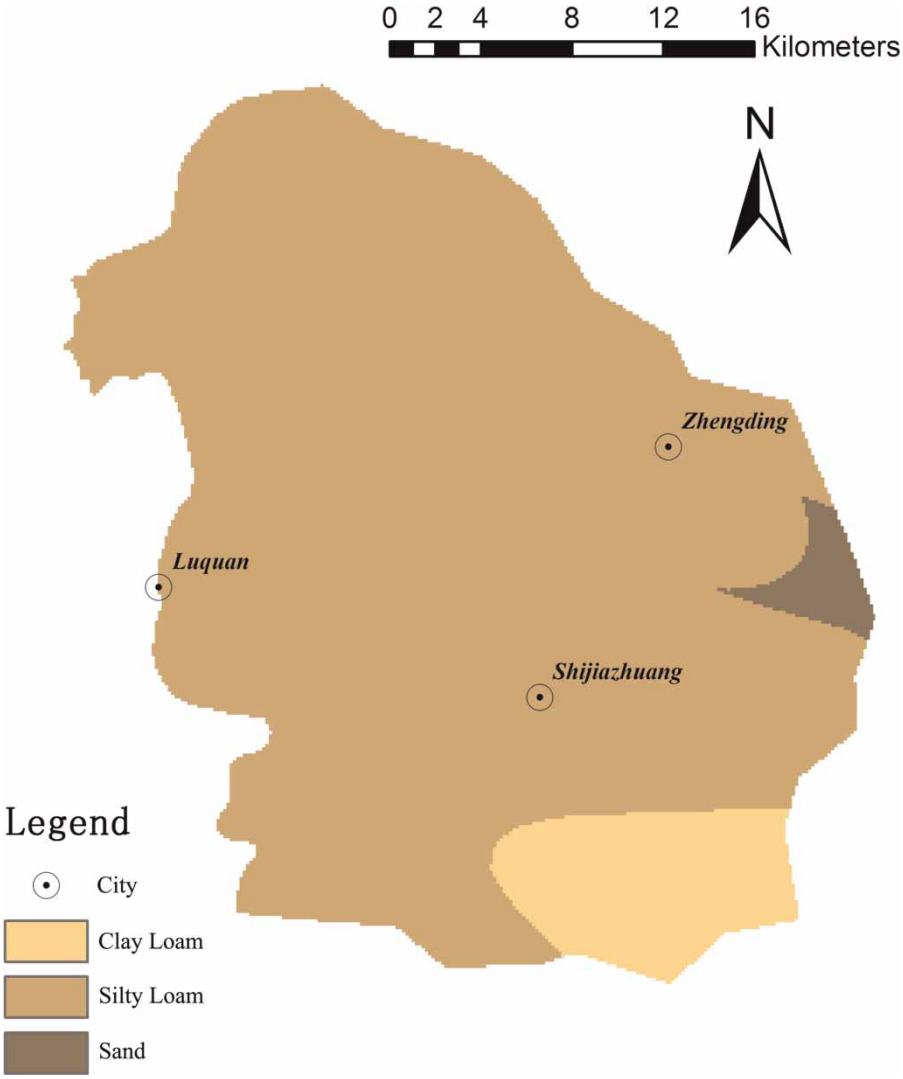

Figure 3 | Soil media (S) distribution map.

extreme precipitation conditions occur less than 8.00% of the years, and the quantities of water that could be used for artificial recharge would be 8.72×10^4 m^3/a and 4.64×10^4 m^3/a, respectively.

Responses of local groundwater levels and net recharge to extreme weather conditions

A groundwater flow simulation model (Du *et al.* 2013) based on GMS (Groundwater Modeling System) software was used to predict groundwater level variation under different extreme weather conditions. The concept of the hydrogeological model has been discussed in detail (Du *et al.* 2013). With extreme scarce conditions, the precipitation has been set as 312.4 mm per year during the prediction period, and the precipitation as 720.2 mm per year during the prediction period under extreme abundant conditions. The two types of precipitation can be calculated based on historical precipitation data, and the frequency of scarce conditions has been set as 87.50% and the frequency of abundant conditions as 12.50%. The extreme precipitations have been applied in the evaluation of groundwater vulnerability variations under artificial recharge (as Scenario 4 and Scenario 5). The amount of artificial recharge

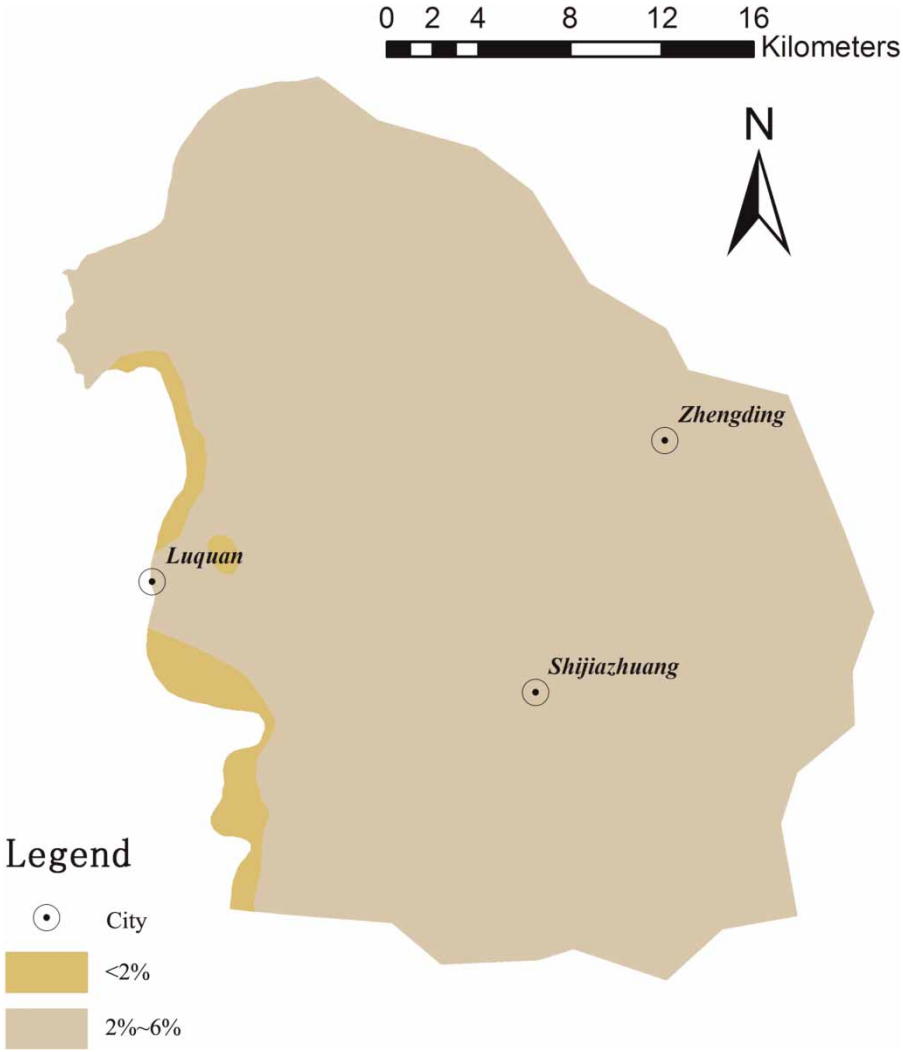

Figure 4 | Topography (T) distribution map.

water has been set as 4.64×10^4 m^3/a and 8.72×10^4 m^3/a, respectively, according to the extreme weather conditions in the HR Basin.

Five scenarios with different weather conditions are proposed.

- Scenario 1: there is no artificial recharge with the present groundwater abstraction status. The groundwater level and distribution of the depth to groundwater table in 2004 are shown in Figures 7(a) and 7(c). The precipitation is an annual average amount of 493 mm per year. Distribution of R is shown in Figure 8(a).
- Scenario 2: there is no artificial recharge with the present groundwater abstraction status. The groundwater level and distribution of the depth to groundwater table in 2013 are shown in Figures 7(b) and 7(d), which is the year before artificial recharge. The precipitation is the annual average amount. Distribution of R is shown in Figure 8(a).
- Scenario 3: there is no artificial recharge with the present groundwater abstraction status. The groundwater level in 2020 could be predicted by the established groundwater simulation model as shown in Figure 9(a). Distribution of the depth to groundwater table is shown in Figure 9(d). The precipitation is the annual average amount. Distribution of R is shown in Figure 8(a).

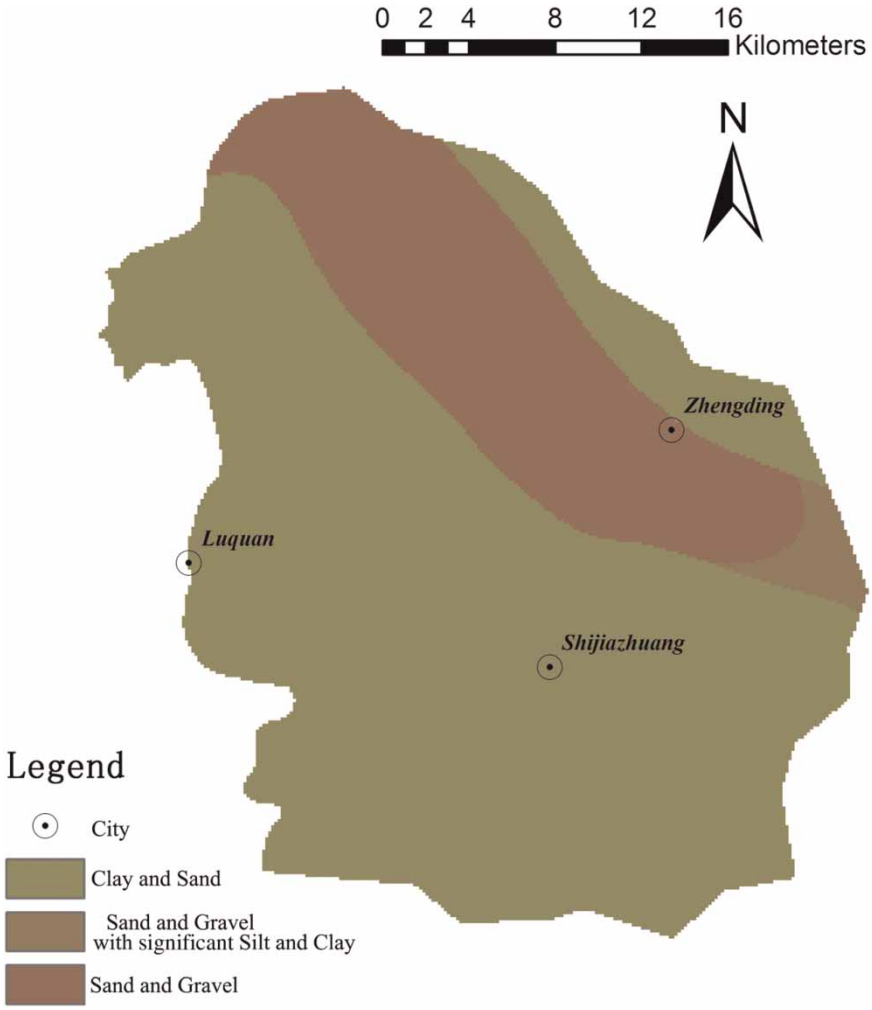

Figure 5 | Vadose zone (I) distribution map.

- Scenario 4: under scarce condition in both HGR and HR, and the quantity that could be used to recharge is 4.64×10^4 m^3/a, and the artificial recharge lasts for 7 years, from 2013 to 2020, with the local groundwater level enhanced as shown in Figure 9(b). Distribution of the depth to groundwater table is shown in Figure 9(e). The precipitation is 312.4 mm per year with a frequency of 12.50%. Distribution of R is shown in Figure 8(b).
- Scenario 5: under abundant condition in both HGR and HR, and the quantity could be used to recharge is 8.72×10^4 m^3/a, and the artificial recharge lasts for seven years, from 2013 to 2020, with the local groundwater level enhanced as shown in Figure 9(c). Distribution of the depth to groundwater table is shown in Figure 9(f). The precipitation is 720.2 mm per year with a frequency of 87.50%. Distribution of R is shown in Figure 8(c).

Responses of groundwater vulnerability to extreme weather conditions

Based on the spatial analysis with GIS method, the DRASTIC model has been used to evaluate the groundwater vulnerability under different conditions. The DRASTIC maps can be seen in Figure 10. The figure shows the following.

(1) High vulnerability area: located at the outlet of the HR rising from the mountain area. The distribution is shown as a strip along the river bed from northwest to

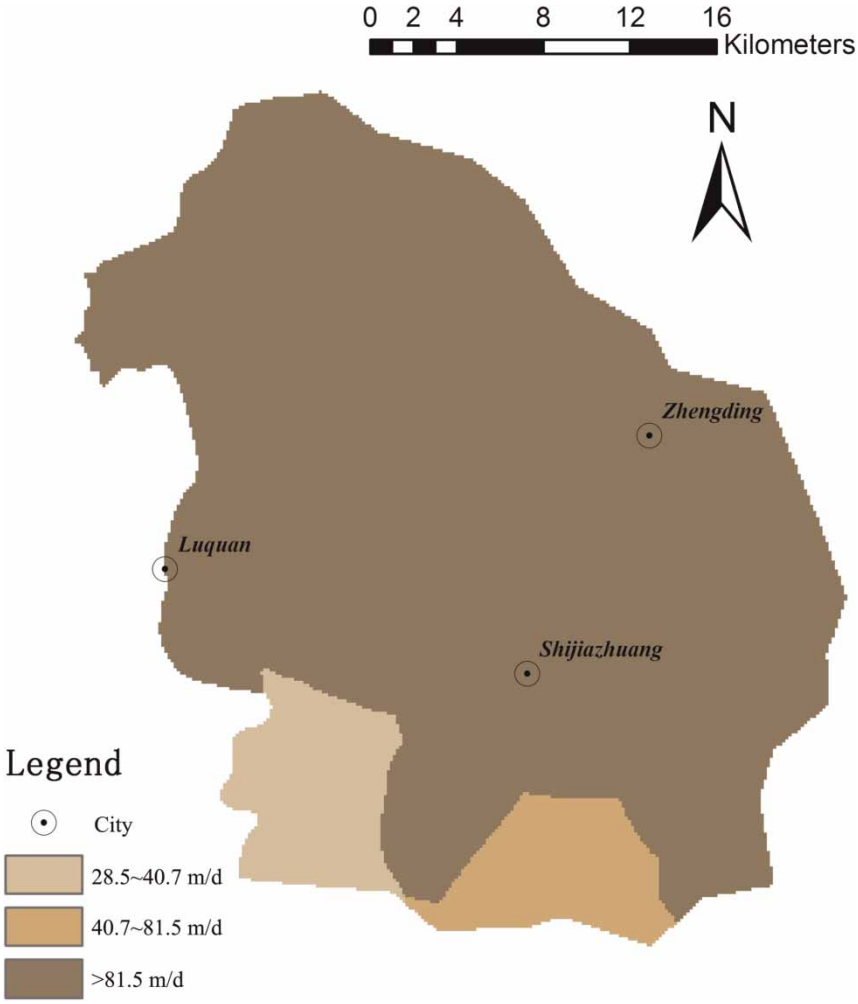

Figure 6 | Hydraulic conductivity (C) distribution map.

Table 3 | Fuzzy probability of abundant-scarce encounters between Han River (HR) and Hutuo River Groundwater Reservoir (HGR) (Du *et al.* 2013)

		HGR			
		A/%	B/%	C/%	Sum/%
HR	I	7.46	9.39	9.10	25.95
	II	12.24	23.77	11.67	47.68
	III	7.10	12.73	6.60	26.43
	Sum/%	26.80	45.89	27.37	100.00

Note: I, II and III refer to abundant, plain, and scarce years of HR, respectively; A, B, and C refer to abundant, plain, and scarce years of HGR, respectively.

southeast, the aquifer permeability is higher and the depth of groundwater level is lower. The net recharge would be higher ascribed to the good infiltration conditions.

(2) Moderate vulnerability area: located at both sides of the high vulnerability area along the HR bed. The aquifer permeability is lower and the depth of groundwater level higher than the high vulnerability area. The DI is proportional to the distances from the river bed.

(3) Low vulnerability area: located at the urban area of Shijiazhuang City. The infiltration conditions are worse, the aquifer permeability is the lowest and the depth of groundwater level the highest.

According to the aforementioned discussion, the local high vulnerability area is located at both sides of the HR bed, low vulnerability at the urban area of Shijiazhuang City, and the other area has moderate vulnerability.

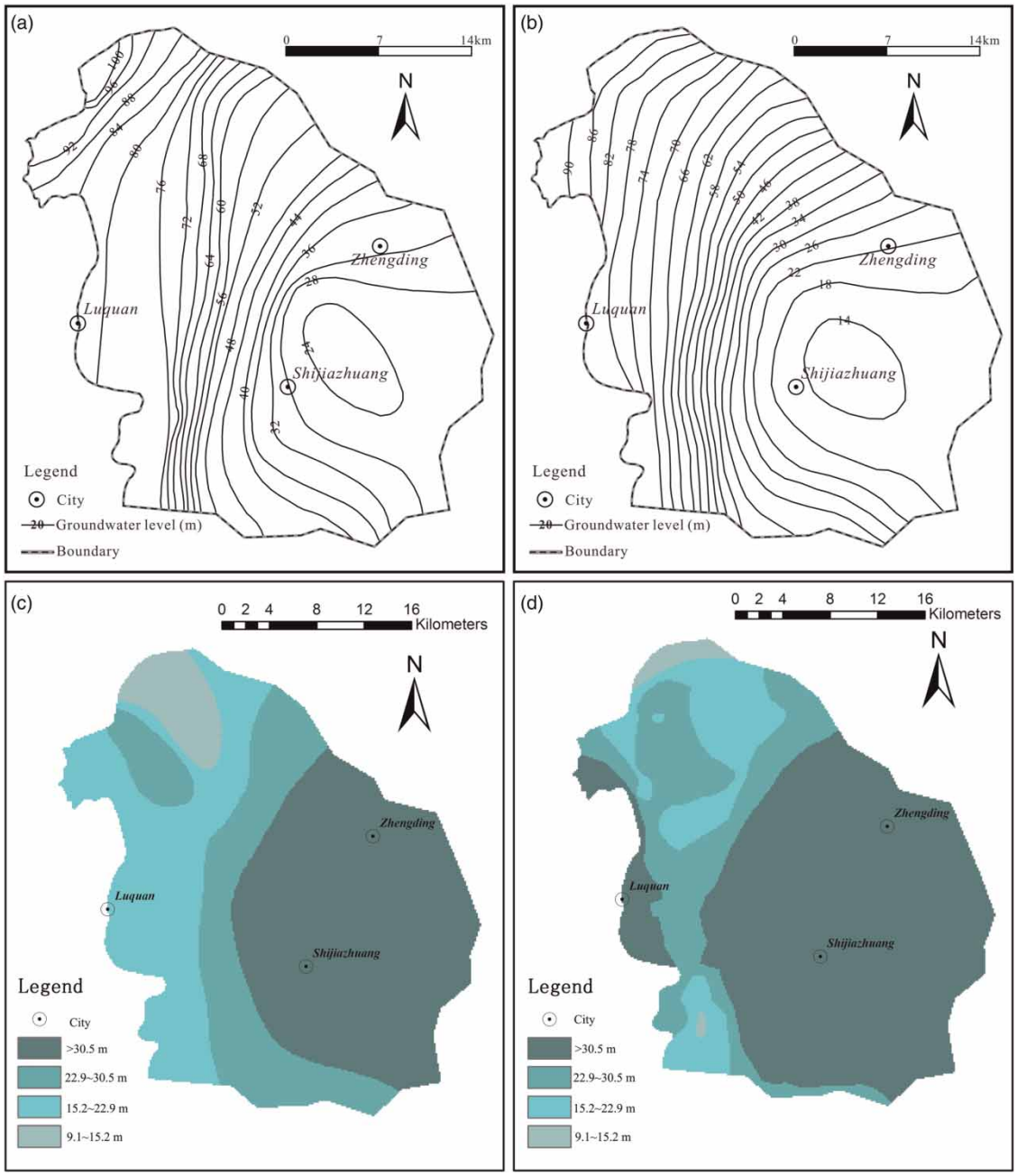

Figure 7 | Groundwater level contour map and the depth to groundwater table distribution map of Scenarios 1 and 2: (a) groundwater level contour map in 2004; (b) groundwater level contour map in 2013; (c) the depth to groundwater table distribution map in 2004; (d) the depth to groundwater table distribution map in 2013.

The area ratios of different vulnerability classes under different conditions are shown in Figure 11. For Scenarios 1, 2, and 3 without artificial recharge and extreme weather conditions, the order of area with different vulnerability classes are moderate > low > high, with the area ratios of moderate class around 47%, and the area ratios of low and high varying between 20 and 30%. Also from the figure it can be seen that the area of moderate class and high class decreased with time, and the area of low class increased with time. This means that the over-exploitation could lowering the depth of groundwater level (D), with a consequent decrease in the local groundwater vulnerability.

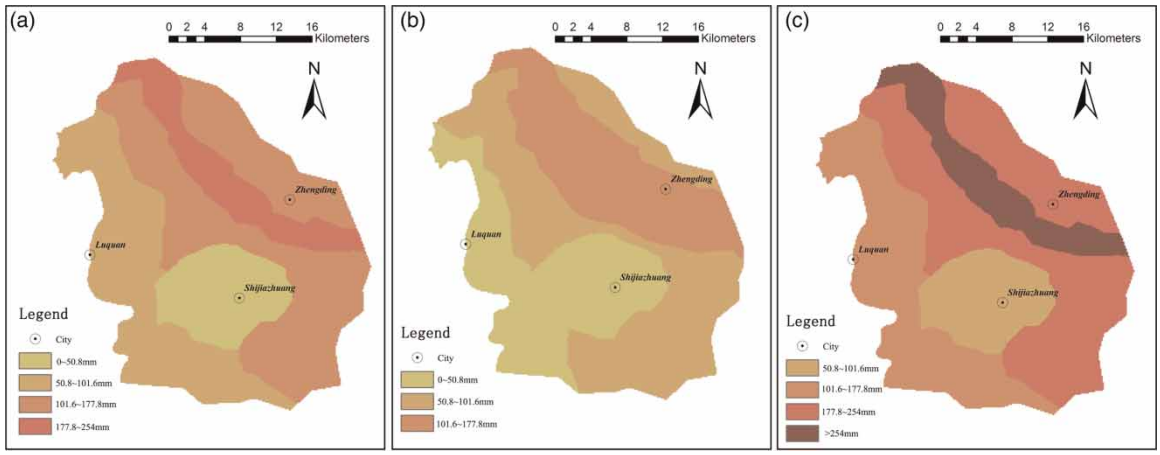

Figure 8 | Net recharge (R) distribution map with different precipitation frequency: (a) precipitation is an annual average amount of 493 mm per year; (b) precipitation is an annual average amount of 312.4 mm per year with precipitation frequency of 87.50%; (c) precipitation is an annual average amount of 720.2 mm per year with precipitation frequency of 12.50%.

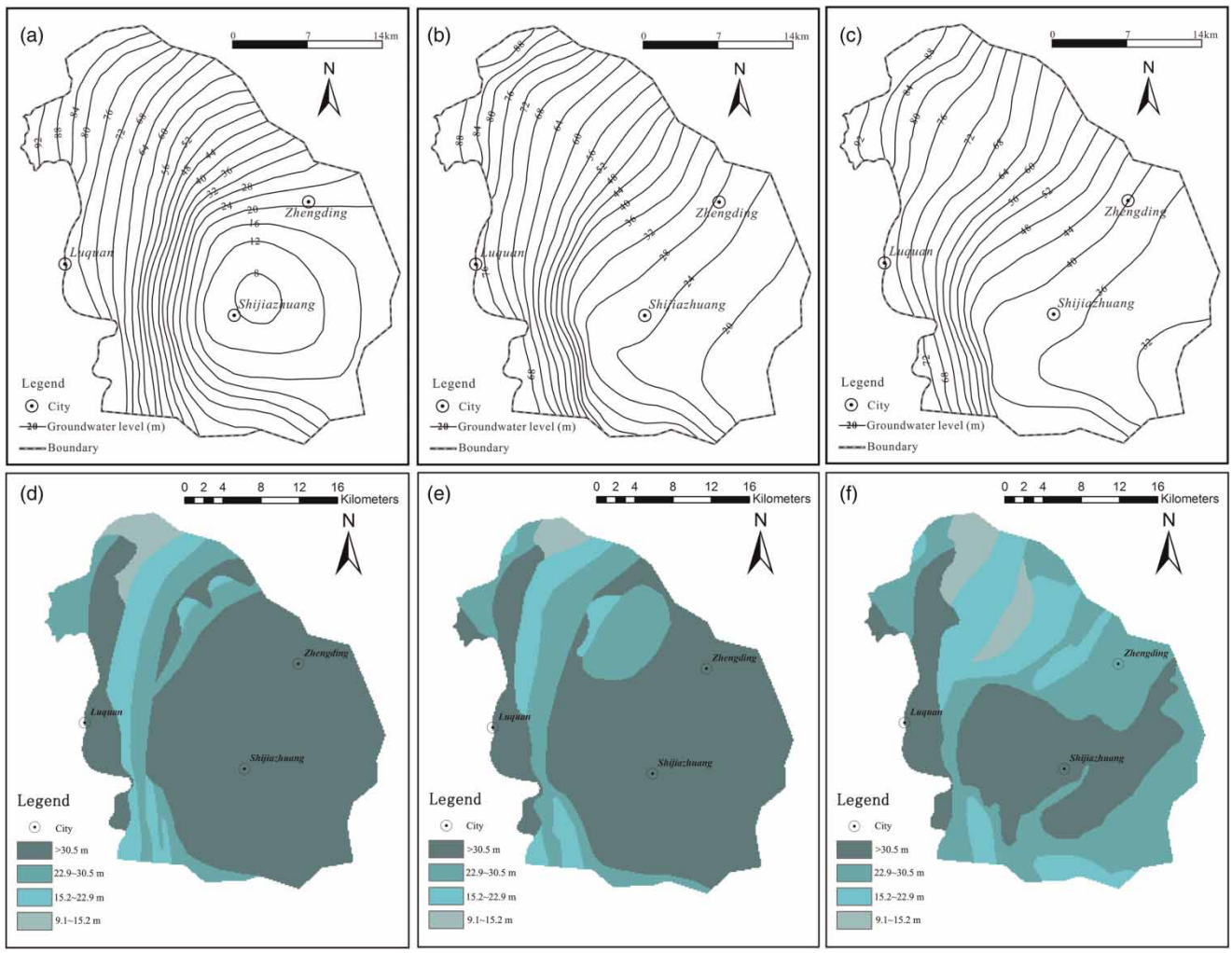

Figure 9 | Groundwater level contour map and the depth to groundwater table distribution map of Scenarios 3 to 5: (a), (b), and (c) are groundwater level contour maps in Scenario 3, Scenario 4, and Scenario 5, respectively; (d), (e), and (f) are the depth to groundwater table distribution maps in Scenario 3, Scenario 4, and Scenario 5, respectively.

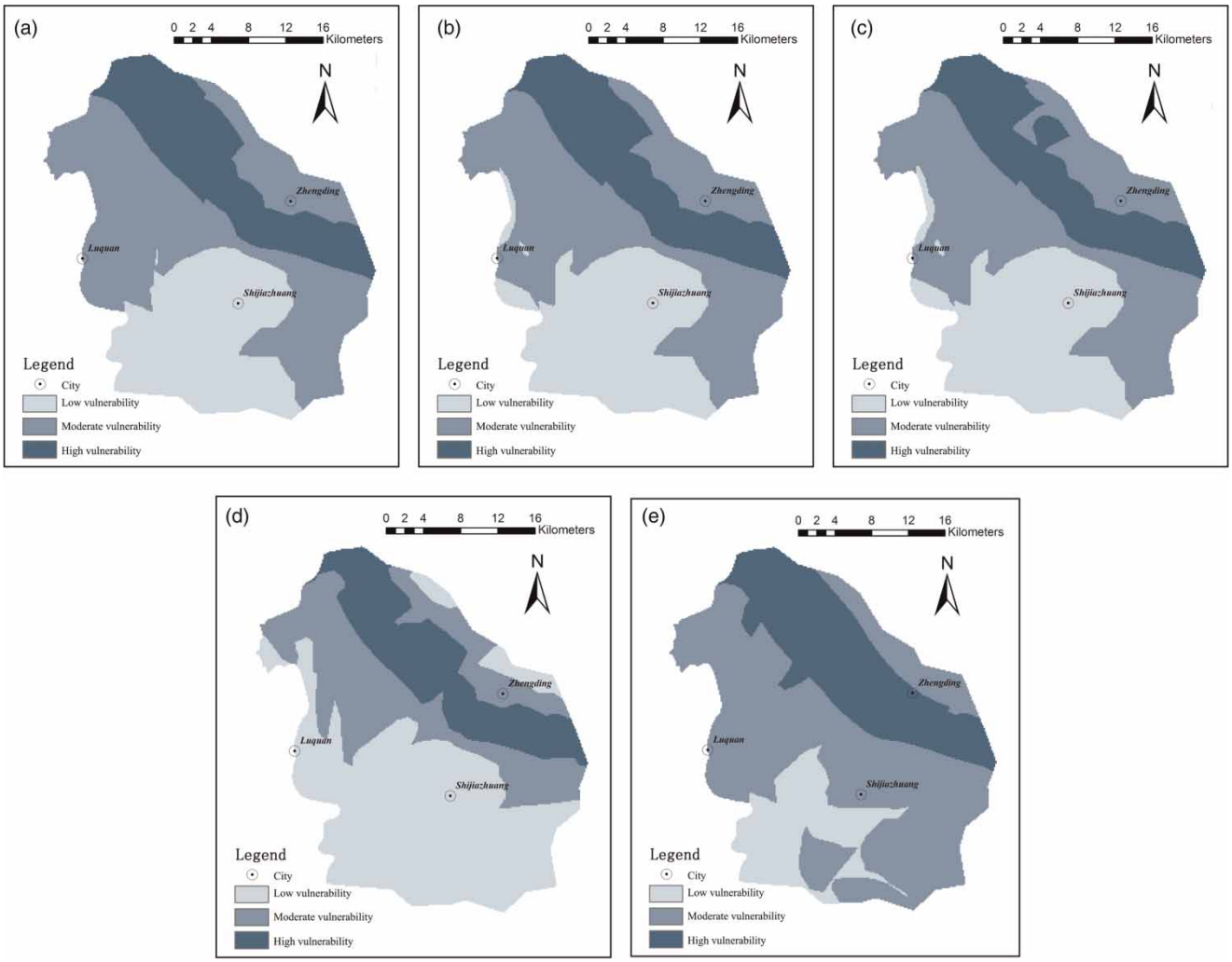

Figure 10 | Groundwater vulnerability evaluation results: (a), (b), (c), (d), and (e) are the results of Scenario 1, Scenario 2, Scenario 3, Scenario 4, and Scenario 5, respectively.

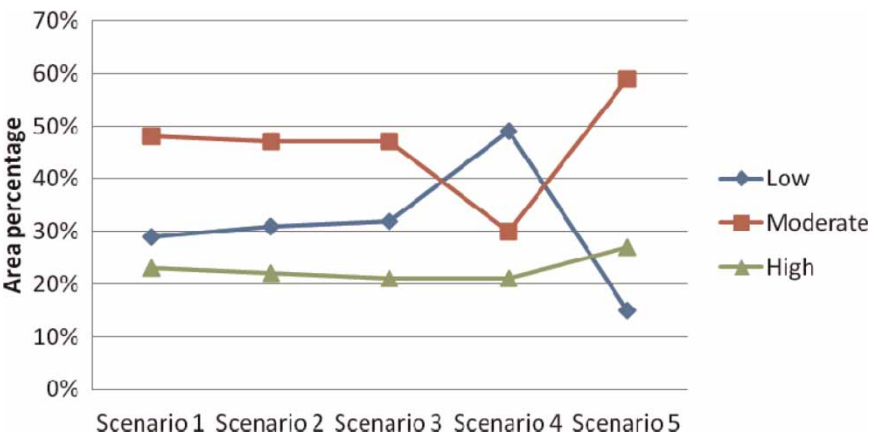

Figure 11 | Area percentage variations of groundwater vulnerability under different scenarios.

From Figure 11, it can be seen that the high vulnerability area keeps static in Scenario 4, but there was an obvious increase for the low vulnerability area and the moderate vulnerability area decreased. This means that the scarce condition in HGR made the precipitation infiltration decrease and the scarce condition in HR made the transferred water for recharge decrease. The induced groundwater level lowering would making the depth of groundwater level (D) increase, and the vulnerability would be lower, ascribed to the conjunctively decreased water quantity of infiltration and artificial recharge.

Comparing Scenario 5 with Scenario 4, the groundwater vulnerability area distribution characteristics show extreme abundant conditions, with the high vulnerability area ratio increasing to 26.78%, the moderate vulnerability area ratio increasing to 58.61%, but the low vulnerability area ratios dropped to 14.61%. This means that with the increasing groundwater level and net recharge under abundant conditions, the decreased D and increased R making the DI increase obviously, the low vulnerability area converted into high or moderate vulnerability area.

CONCLUSIONS

(1) Simultaneously abundant years of the local area and Han River Basin is 7.46% of the years, and 6.60% of the years with simultaneously scarce years. Both of the extreme precipitation conditions would occur less than 8.00% of the years, and the quantities of water that could be used for artificial recharge would be $8.72 \times 10^4\ m^3/a$ and $4.64 \times 10^4\ m^3/a$, respectively.

(2) Five scenarios with artificial recharge conditions and extreme weather conditions have been discussed, and the DRASTIC evaluation maps indicate that the groundwater vulnerability would not change a great deal without extreme conditions under artificial recharge. Under extreme scarce conditions (Scenario 4), the induced groundwater level lowering would make the depth of groundwater level (D) increase, and the vulnerability would be lower, ascribed to the conjunctively decreased water quantity of infiltration and artificial recharge. Under extreme abundant conditions (Scenario 5), the decreased depth of groundwater level (D) and increased net recharge (R) would make the vulnerability increase obviously, with the low vulnerability area being converted into the moderate and high vulnerability areas.

(3) More attention should be paid to the quality of recharged water and monitoring schemes should be carried out during the running period around the infiltration field, which could be useful to protect the groundwater resources and enhance the security of water supply in Shijiazhuang City.

ACKNOWLEDGEMENTS

X. Su and W. Xu contributed to this work equally. This work was supported by the Chinese National Science Fund Project (NSFC41073054).

REFERENCES

Aller, L., Lehr, J. H. & Petty, R. 1987 Drastic – a standardized system to evaluate groundwater pollution potential using hydrogeologic setting. *J. Geolog. Soc. India* **29** (1), 23–37.

Aschonitis, V. G., Mastrocicco, M., Colombani, N., Salemi, E., Kazakis, N., Voudouris, K. & Castaldelli, G. 2012 Assessment of the intrinsic vulnerability of agricultural land to water and nitrogen losses via deterministic approach and regression analysis. *Water Air Soil Pollut.* **223**, 1605–1614.

Baalousha, H. 2006 Vulnerability assessment for the Gaza Strip, Palestine using DRASTIC. *Environ. Geol.* **50**, 405–414.

Bai, L. P., Wang, Y. Y. & Meng, F. S. 2012 Application of DRASTIC and extension theory in the groundwater vulnerability evaluation. *Water Environ. J.* **26**, 381–391.

Barbash, J. E. & Resek, E. A. 1996 *Pesticides in Ground Water: Distribution, Trends, and Governing Factors.* Pesticides in the Hydrologic System series, 2. Ann Arbor Press, Chelsea, Michigan, 590 pp.

Bouwer, H. 2002 Artificial recharge of groundwater: Hydrogeology and engineering. *Hydrogeol. J.* **10**, 121–142.

Chen, S. K., Jang, C. S. & Peng, Y. H. 2013 Developing a probability-based model of aquifer vulnerability in an agricultural region. *J. Hydrol.* **486**, 494–504.

Dong, W. H., Kang, B., Du, S. H. & Shi, X. F. 2013 Estimation of shallow groundwater ages and circulation rates in the Henan Plain, China: CFC and deuterium excess methods. *Geosci. J.* doi:10.1007/s12303-013-0037-8.

Du, S. H., Su, X. S. & Zhang, W. J. 2013 Effective storage rates analysis of groundwater reservoir with surplus local and

transferred water used in Shijiazhuang City, China. *Water Environ. J.* **27**, 157–169.

Huan, H., Wang, J. S. & Teng, Y. G. 2012 Assessment and validation of groundwater vulnerability to nitrate based on a modified DRASTIC model: a case study in Jilin City of Northeast China. *Sci. Total Environ.* **440**, 14–23.

Iqbal, J., Gorai, A. K., Poonam, T. & Gopal, P. 2012 Approaches to groundwater vulnerability to pollution: a literature review. *Asian J. Water Environ. Pollut.* **9**, 105–115.

Li, Y. G. 2007 *Groundwater Reservoir Construction Research*. China Environmental Science Press, Beijing.

Qian, J., Zhan, H. B., Wu, J. F. & Chen, Z. 2009 What can be learned from sequential multi-well pumping tests in fracture-karst media? A case study in Zhangji, China. *Hydrogeol. J.* **17**, 1749–1760.

Ramos, L. J. A., Noyola, M. C., Tapia, S. F. O., García, J. T. S. & Gutiérrez, L. R. R. 2012 Assessing the inconsistency between groundwater vulnerability and groundwater quality: the case of Chapala Marsh, Mexico. *Hydrogeol. J.* **20**, 591–603.

Robins, N. S. 1998 Recharge: the key to groundwater pollution and aquifer vulnerability. In: *Groundwater Pollution, Aquifer Recharge and Vulnerability* (N. S. Robins, ed.). Special Publications 130, Geological Society, London, pp. 1–5.

Saidi, S., Bouri, S., Dhia, H. B. & Anselme, B. 2011 Assessment of groundwater risk using intrinsic vulnerability and hazard mapping: application to Souassi Aquifer, Tunisian Sahel. *Agric. Water Manage.* **98**, 1671–1682.

Su, X. S., Xu, W. & Du, S. H. 2013 In situ infiltration test using a reclaimed abandoned river bed: managed aquifer recharge in Shijiazhuang City, China. *Environ. Earth Sci.* doi: 10.1007/s12665-013-2893-y.

Sundaram, V. L. K., Dinesh, G., Ravikumar, G. & Govindarajalu, D. 2008 Vulnerability assessment of seawater intrusion and effect of artificial recharge in Pondicherry Coast Region using GIS. *Ind. J. Sci. Technol.* **1**, 1–7.

Worrall, F. & Kolpin, D. W. 2004 Aquifer vulnerability to pesticide pollution combining soil, land-use and aquifer properties with molecular descriptors. *J. Hydrol.* **293**, 191–204.

Zhai, Y., Guo, Y., Zhou, J., Guo, N., Wang, J. & Teng, Y. 2013 The spatio-temporal variability of annual precipitation and its local impact factors during 1724–2010 in Beijing, China. *Hydrol. Process.* doi:10.1002/hyp.9772.

First received 12 July 2013; accepted in revised form 28 September 2013. Available online 26 November 2013